Research on Chemical Intermediates
https://doi.org/10.1007/s11164-018-3521-y

A ternary hybrid system based on combination of mesoporous silica, heteropolyacid and double-layered clay: an efficient catalyst for the synthesis of 2,4-dihydro-3*H*-pyrazol-3-ones and pyranopyrazoles in aqueous medium: studying the effect of the synthetic procedure on the catalytic activity

Samahe Sadjadi[1] · Majid M. Heravi[2] · Vahideh Zadsirjan[2] · Vahid Farzaneh[1]

Received: 16 October 2017 / Accepted: 2 July 2018

Abstract

SBA/hydrotalcite/heteropolyacid nanocomposite is synthesized via a novel procedure in which the as-prepared heteropolyacid-loaded SBA-15 was impregnated with calcined hydrotalcite. The ternary hybrid system was characterized by using SEM/EDS, XRD, BET, TPD, TGA, FTIR and ICP-AES and also used as an efficient catalyst for the synthesis of 2,4-dihydro-3*H*-pyrazol-3-one derivatives via the reaction of arylaldehydes and 5-methyl-1*H*-pyrazol-3(2*H*)-one under reflux condition. Moreover, the catalytic activity of this catalyst was confirmed for the one-pot four-component reaction of aryl aldehydes, ethylacetoacetate, malononitrile and hydrazine hydrate/phenyl hydrazine in aqueous media for the synthesis of pyranopyroles. The investigation of the effect of the synthetic procedure and calcination of the hydrotalcite on the catalytic activity of the catalyst established that this factor does not exert a marked effect on the catalytic activity. The present procedures benefit from diverse advantages, including high yields, simplicity, mild reaction conditions and short reaction times. Moreover, this catalyst was reusable for up to five reaction runs and the HPA leaching was suppressed.

Keywords 2,4-Dihydro-3*H*-pyrazol-3-ones · Pyranopyrazoles · Catalyst · Hybrid · Heteropolyacid · SBA · Hydrotalcite

Electronic supplementary material The online version of this article (https://doi.org/10.1007/s11164-018-3521-y) contains supplementary material, which is available to authorized users.

Extended author information available on the last page of the article

Published online: 07 July 2018

Introduction

Mesoporous silica materials such as SBA-15 exhibit outstanding properties, including non-toxicity, good mechanical properties, thermal stability and tunability. The utility of these compounds for a broad range of applications [1, 2] such as catalysis [3], gas storage and waste treatment has been proved. Among various uses, catalysis is of great importance. There are numerous reports on the catalytic activities of mesoporous compounds [4–8]. In the last decade, functionalization of mesoporous silica materials as well as designing hybrid catalytic systems based on functionalized compounds has attracted growing attention and various catalytic species such as complexes [9, 10], nanoparticles [11, 12] and heteropolyacids [13] have been incorporated in mesoporous silica material hybrid catalysts. For this purpose, heteropolyacids (HPAs) are considered as promising candidates due to their unique features such as non-toxicity, Bronsted acidity, redox potentiality and non-corrosive nature [14]. Moreover, these catalysts exhibit high catalytic activities for various photochemical, organic [15], electrochemical [16] and petrochemical [17] reactions. The merit of incorporating HPA into the mesoporous silica materials is transforming homogenous HPAs [14] into heterogeneous catalyst and improving the catalyst surface area.

Layered double hydroxides (LDHs) are two-dimensional layered materials in which the layers are composed of two types of metallic cations and the interlayer space hosts anionic species. The general formula of an LDH is $[M^{2+}_{1-x}M^{3+}_{x}(OH)_2]^{x+}A^{n-}_{x/n}\cdot mH_2O$, where M^{2+} and M^{3+} are di- and trivalent metal ions, A^{n-} is the interlayer anion and x is the fraction of M^{2+}, i.e. $x = M^{2+}/(M^{2+} + M^{3+})$ [18, 19]. These layered materials have various applications, including catalysis [20–22], polymer science and designing carrier systems [23], emerged from their unique properties such as ion exchange ability, tunable element compositions, and acid–base properties.

One-pot multicomponent reactions (MCRs) provide a potent class of synthetic procedures because of their excellent efficiencies, short reaction times and distinctive selectivity [24–26]. These reactions create one of the best pathways for modern organic chemistry since they can employ most of the component atoms of diverse reactant compounds to provide a target product [27, 28]. Green chemistry processes follow to develop alternative methods which help to protect properties and decrease costs. The replacement of usual solvents with H_2O that is harmless to health and is accessible in large amounts is a significant basic method [29, 30]. Also, organic synthesis in water gives main benefits, involving rate improvement and insolubility of the target molecules that assists their separation through simple filtration [26].

Heterocycles bearing pyrazole rings are remarkable target products in synthetic and medicinal chemistry since this ring is a vital scaffold in numerous biologically active molecules. Pyrazole is an essential heterocycle analogue that demonstrates a significant role in various pharmaceutical and agrochemical industries [31]. Among this group of molecules, 2,4-dihydro-3*H*-pyrazol-3-one derivatives have a wide range of biological properties involving antibacterial, antipyretic, antidepressant and

anti-inflammatory activities [32]. Furthermore, they are imperative intermediates in organic chemistry [33]. The treatment of aldehydes with 3-methyl-1-phenyl-5-pyrazolone is a useful pathway to make 4,4′-(arylmethylene)bis(1*H*-pyrazol-5-ols). Diverse catalysts have been applied for the synthesis of these products through the condensation reaction. These catalysts contain sodium dodecyl sulfate [34], piperidine or acetic acid [35] silica-bonded S-sulfonic acid [36], ETBA [37] and CAN [38].

Pyranopyrazoles are fused heterocyclic molecules that contain various biological activities, including bactericidal [39], fungicidal [40] and vasodilatory activities [41], and act as anticancer agents [42]. Pyranopyrazole was first provided by the treatment between 3-methyl-1-phenylpyrazolin-5-one and tetracyanoethylene [43]. Sharanin and co-workers demonstrated a one-pot and three-component reaction between aromatic aldehyde, pyrazolone and malononitrilein under Et_3N as a catalyst in EtOH to provide pyranopyrazoles [44]. Also, in this route, Vasuki and Kandhasamy and co-workers reported a four-component reaction of aldehydes, ethyl acetoacetate, malononitrile and hydrazine hydrate in H_2O and catalytic β-cyclodextrin [45].

In the following of our research on developing new catalysts for improving organic transformations under green and eco-friendly condition [46, 47], we recently reported the catalytic utility of SBA-15/hydrotalcite nanocomposite for immobilization of HPA [48]. The hybrid system was prepared through formation and functionalization SBA-15 followed by incorporation of HPA and subsequent synthesis of un-calcined LDH in the presence of HPA-loaded SBA-15. To expand our research on the catalytic potency of ternary hybrid of SBA/LDH/HPA and because of the significance of pyrazolone derivatives, herein we disclose a novel procedure for the synthesis of SBA/LDH/HPA nanocomposite through impregnation of HPA-loaded SBA-15 and calcined LDH and studied its catalytic activity for the synthesis of 2,4-dihydro-3*H*-pyrazol-3-ones and pyranopyrazole derivatives. Furthermore, to provide more insight into the effect of the synthetic procedure and use of calcined LDH on the catalytic activity, the catalytic activity of this catalyst is compared with that prepared via our previously reported methodology, synthesis of un-calcined LDH in the presence of HPA-loaded SBA-15 [48]. Noteworthy, the catalyst reusability and HPA leaching are investigated too.

Results and discussion

Catalyst characterization

The FTIR spectrum of the catalyst is illustrated in Fig. 1. This spectrum shows two main characteristic bands. One, the bands related to the SBA-15 structure, i.e. the bands at 3450 and 1631 cm^{-1} that can be representative of SiO–H and the adsorbed water respectively as well as the bands at 1084, 797, 950 and 454 $cm^{-1,}$ which are assigned to stretching of Si–O–Si. Notably, the three mentioned peaks can also be assigned to the symmetric stretching of P–O, W–Oc–W, W–Oe–W and W–Ot, respectively [50].

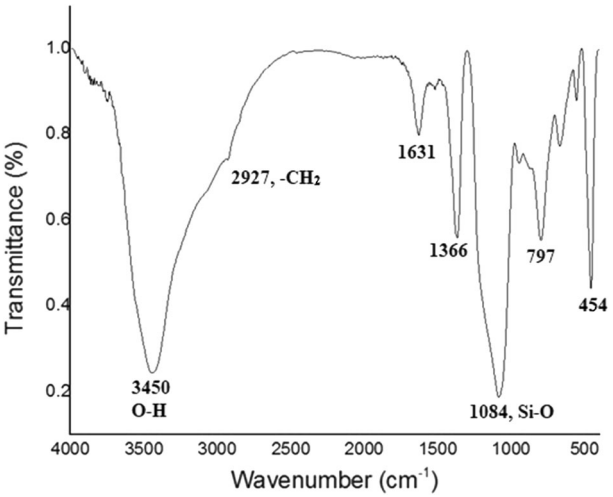

Fig. 1 FTIR spectrum of the catalyst

Noteworthy, the band at 2927 cm^{-1} is representative of the $–CH_2$ stretching and clearly establish the conjugation of APTES to SBA-15. The second characteristic band is the band observed at 1366 cm^{-1} which is representative of LDH scaffold [51].

The SEM/EDX images of the hybrid catalyst are depicted in Fig. 2. As depicted, the SEM images of the hybrid system are distinguished from those of pure SBA-15 (Fig. 2). The hybrid system exhibited less compact morphology in which the rod-like morphology of pure SBA-15 is observable to some extent. This observation confirmed that incorporation of calcined LDH can alter the morphology of the SBA-15. Notably, the SEM images of SBA/LDH/HPA and SBA/LDH/HPA/P (Fig. 1 in supporting information) [48] are distinguished, indicating that the synthetic procedure and use of calcined LDH affect the morphology of final composite. The catalyst prepared by using calcined LDH exhibited more packed morphology.

Although the EDX analysis cannot prove the formation of LDH, SBA-15 and incorporation of HPA, it can be considered as a useful tool for confirming the results obtained from other analyses. As shown in Fig. 2, the Si and O atoms are present in the structure. This may indicate the formation of SBA-15 structure. Besides, the C and N atoms can be assigned to the attachment of APTES. Furthermore, the observation of Al, Mg and O atoms can be representative of LDH framework. The presence of P and W atoms can prove the immobilization of HPA.

The low-angle and wide-angle XRD patterns of the nanocomposite are shown in Fig. 3. This pattern which contained three peaks at 0.9°, 1.5° and 1.8° established 100, 110 and 200 reflections of the highly ordered periodic arrangement of hexagonal channels and also is in good accordance with previously reported XRD patterns for SBA-15 [52]. This observation confirmed that upon formation of nanocomposite, the ordered structure of SBA-15 was not destroyed. The peaks observed in the wide-angle XRD pattern of the catalyst are in good agreement with

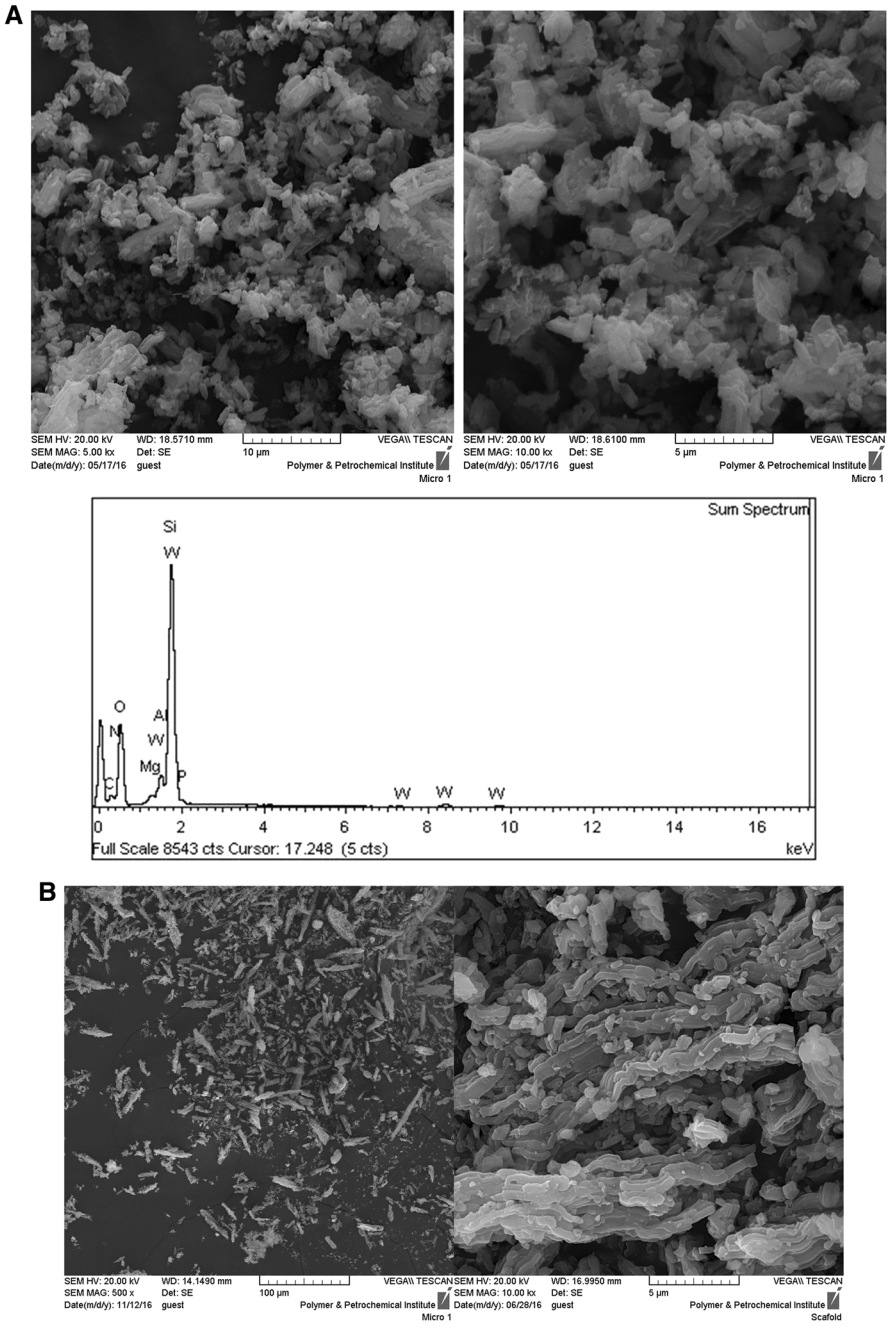

Fig. 2 **a** SEM/EDX images of the catalyst, **b** SEM images of pure SBA-15 [48]

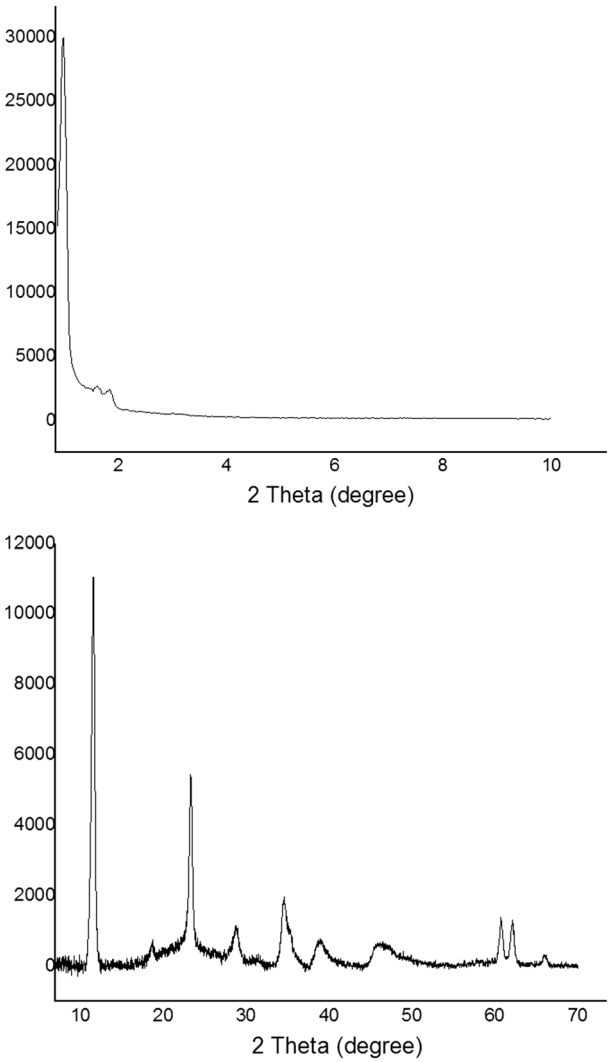

Fig. 3 The low-angle (top) and wide-angle (bottom) XRD patterns of the catalyst

the previous reports and clearly indicate the formation of LDH framework [53, 54]. Comparing with SBA/LDH/HPA/P [48], the wide-angle XRD pattern of SBA/LDH/HPA is completely different (Fig. 2 in supporting information). The XRD pattern of the former, un-calcined LDH showed only the layered structure, while the SBA/LDH/HPA XRD pattern exhibited sharp and symmetric reflections for (003), (006), (110) and (113) planes with broad and asymmetric reflections for (012), (015) and (018) planes [55]. It is worth mentioning that no distinguished peak was observed in the XRD pattern for HPA. Based on a previous report, this can be attributed to uniform and high dispersion of the HPA as well as its low amount [56].

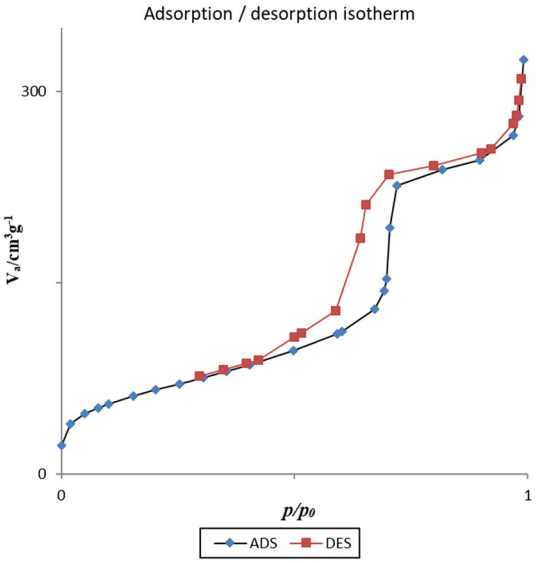

Fig. 4 Nitrogen adsorption–desorption isotherm of the LDH/SBA/HPA

Next, to study the textural properties of LDH/SBA/HPA, a nitrogen adsorption–desorption isotherm of the LDH/SBA/HPA was recorded (Fig. 4). The shape of the obtained isotherm confirmed the porous structure of the catalyst and belonged to the type IV isotherms with a H2-type hysteresis loop. Notably, the nitrogen adsorption–desorption isotherms of the LDH/SBA/HPA and LDH/SBA/HPA/P were similar and indicative of porous structures (Fig. 3 in supporting information). The BET surface area of the hybrid system ($\sim$ 200 m^2 g^{-1}) was lower that of free SBA-15 ($\sim$ 700 m^2 g^{-1}) and higher than that of LDH ($\sim$ 100 m^2 g^{-1}).

To estimate the value of HPA in the ternary hybrid system, LDH/SBA/HPA was digested in concentrated HCl and HNO_3 solution and the obtained extract was analyzed by using ICP-AES analysis. Using this procedure, the content of HPA was measured to be about 5.5 w/w%.

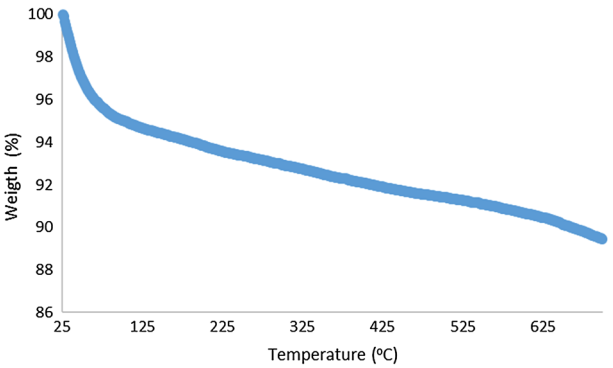

Fig. 5 TGA analysis of the catalyst

A TGA thermogram of LDH/SBA/HPA is illustrated in Fig. 5. As depicted, two degradation stages can be observed over the range of 25–700 °C. The first degradation step which occurred at about 100 °C is attributed to the loss of adsorbed water molecules. The next degradation step was observed at about 400 °C (∼ 3 wt%) and can be assigned to the loss of silane functionality of SBA-15.

The acidity of the catalyst was studied by measuring the temperature-programmed desorption of NH_3 (NH_3-TPD, Fig. 6). As shown, the catalyst exhibited two broad peaks distributed in the region of ∼ 100, 200 to 400 °C, implying two types of acid sites in the catalyst.

According to the literature, the low-temperature desorption peak observed at ∼ 100 °C indicates the presence of weak acidic sites on the catalyst. The high-temperature desorption peak (detected at 400 °C), on the other hand, can confirm the strong acidic sites on the catalyst. These sites can be due to the incorporation of HPA [57, 58].

Catalytic activity

The catalytic activity of the novel hybrid catalyst was examined for the development of 4,4′-alkylmethylene-bis(3-methyl-5-pyrazolones) via the treatment of 5-methyl-1*H*-pyrazol-3(2*H*)-one and aldehyde in aqueous media under reflux condition (Scheme 1). At first, the reaction of 5-methyl-1*H*-pyrazol-3(2*H*)-one and bezaldehyde was considered as a model reaction to examine the catalytic potential of the designed catalyst and determine the optimum reaction condition. Initially, the model reaction was performed in the absence of the catalyst. The result established that the yield of the desired product in this condition was low, indicating the necessity of using catalyst for this organic transformation. Secondly, the catalytic activity of the hybrid system was compared with each component individually, i.e. SBA, HPA and LDH. The results demonstrated that the ternary nanocomposite exhibited superior catalytic activity compared to each component. Next, to study whether the synthetic procedure of SBA/LDH/HPA and using calcined LDH can affect the catalytic activity, the model reaction was performed in the presence of SBA/LDH/HPA and SBA/LDH/HPA/P. Interestingly, the results established that

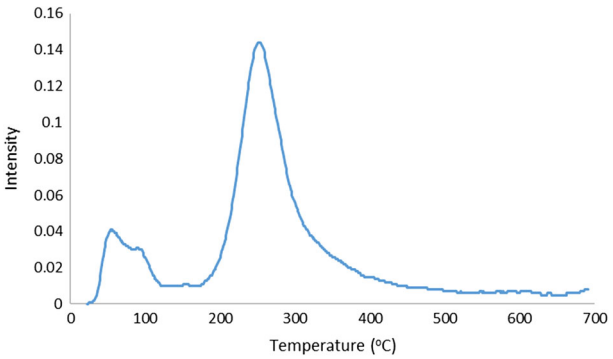

Fig. 6 NH_3-TPD of the catalyst

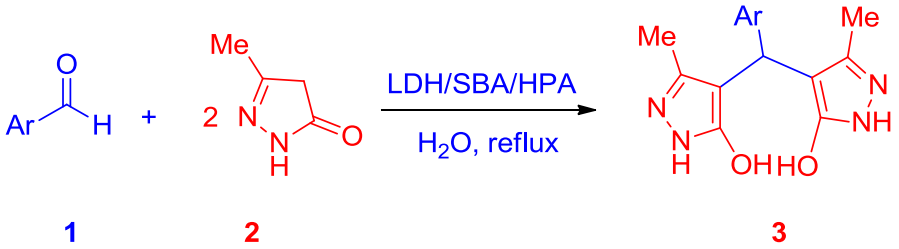

Scheme 1 Synthesis of 4,4′-alkylmethylene-bis(3-methyl-5-pyrazolones) derivatives **3** under LDH/SBA/HPA as an efficient catalyst

despite different physical characteristics, both catalysts exhibited similar catalytic activity. This observation can confirm that in the nanocomposite, the catalytic activity of the LDH component is independent of its calcined or un-calcined nature and both of them exhibited similar catalytic activities.

Next, to optimize the reaction conditions, a series of experiments with diverse solvents and quantities of the catalyst was accomplished. As shown, the best yield of the desired product was achieved in water as solvent and in the presence of 5 mg of catalyst under reflux condition in water after 15 min (Table 1). Then, to establish the generality of the method, the optimum reaction condition was applied for the synthesis of various derivatives of 4,4′-alkylmethylene-bis(3-methyl-5-pyrazolones). As demonstrated in Table 2, this procedure exhibited broad substrate scope in which diverse aldehydes with electron-withdrawing and electron-donating groups can be employed effectively to furnish the target products in high yields. As anticipated, the aldehydes containing electron-withdrawing groups led to the desired products in slightly higher yields.

Table 1 Optimizing the reaction conditions for the synthesis of **3a**[a]

Entry	Catalyst amount (mg)	Solvent	Temperature	Yield (%)
1	–	Water	Reflux	Trace
2	5	Water	r.t.	20
3	5	Water	Reflux	85
4	5	CH_3CN	Reflux	60
5	5	DMF	Reflux	55
6	5	EtOH	Reflux	80
7	5	Toluene	Reflux	50
8	2	Water	Reflux	70
9	3	Water	Reflux	78
10	7	Water	Reflux	85

[a]Isolated yield

Table 2 LDH/SBA/HPA-mediated synthesis of 4,4′-alkylmethylene-bis(3-methyl-5-pyrazolones) derivatives

Entry	Product	Ar	Yield (%)[a]	mp (°C) found	mp (°C) from lit. [34]
1	**3a**	C_6H_5	85	229–231	230–232
2	**3b**	4-HOC_6H_4	79	263–265	262–264
3	**3c**	4-ClC_6H_4	82	225–227	224–226
4	**3d**	3-$NO_2C_6H_4$	87	270–273	271–272
5	**3e**	4-$NO_2C_6H_4$	90	299–302	300–302

[a]Yields refer to isolated products

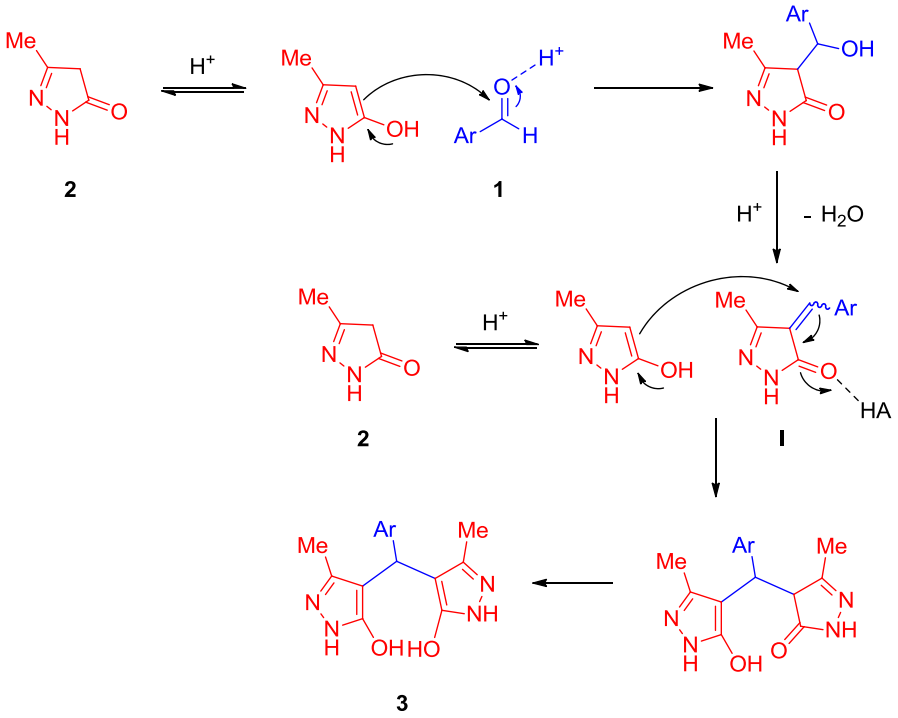

Scheme 2 Plausible mechanism for the synthesis of 4,4′-(arylmethylene)bis(3-methyl-1*H*-pyrazol-5-ols)

Reaction mechanism for the synthesis of 4,4′-alkylmethylene-bis(3-methyl-5-pyrazolones)

A probable mechanism for the synthesis of 4,4′-(arylmethylene)bis(3-methyl-1*H*-pyrazol-5-ols) is exhibited in Scheme 2. The catalyst showed an important role in improving the electrophilic character of the electrophiles in the reaction. The reaction happens through initial construction of the intermediate I, produced by Knoevenagel condensation reaction of the first equivalent of an enolic form of

3-methyl-1*H*-pyrazol-5(4*H*)-one, **2,** and aryl aldehydes, **1**, that reacted successively with a second equivalent of an enolic form of **2** to give the corresponding products **3**.

Motivated by the gratifying results for the synthesis of 2,4-dihydro-3*H*-pyrazol-3-ones derivatives and with the aim of expanding the catalytic utility of the ternary hybrid system, we studied the catalytic activity of novel catalyst for promoting the four-component reaction of aromatic aldehydes, ethylacetoacetate, malononitrile and hydrazine hydrate/phenylhydrazine for the synthesis of pyranopyrazoles (Scheme 3). Again, the comparison of the catalytic activities of SBA/LDH/HPA and SBA/LDH/HPA/P confirmed their equal catalytic activity. For a detailed exploration, the reaction between ethyl acetoacetate, hydrazine hydrate, benzaldehyde and malononitrile was considered as a model reaction and applied for the optimization of reaction conditions; for this purpose, various solvents and catalyst amounts were tested. Noteworthy, the reaction was not accomplished in the absence of the catalyst. The results demonstrated the water was the solvent of choice. Furthermore, the optimum amount of the catalyst was found to be 5 mg (Table 3).

In order to establish the generality of this procedure, the catalyst was employed for the treatment of diverse aryaldehydes with ethylacetoacetate, malononitrile and hydrazine hydrate/phenylhydrazine (Table 4). The method displayed good substrate tolerance and the application of different electron-deficient and electron-rich aldehydes resulted in the desired products in excellent yields.

To further generalize this protocol, biologically active spiro compounds were also synthesized from four-component reaction of isatin, malononitrile and 3-methyl-1*H*-pyrazol-5(4*H*)-one (Scheme 4). The result established that the spiro derivative can also be synthesized in high yield and short reaction time (Table 4, entry 13).

Reaction mechanism for the synthesis of pyranopyrazoles

A probable mechanism can be reasonably suggested for the development of pyranopyrazole **6** from the reaction of benzaldehyde, hydrazine hydrate, malononitrile and ethyl acetoacetate (Scheme 5). In this pathway, the basic site of LDH/SBA/HPA, i.e. LDH, plays a key role in the improving the activity of the reagents for the synthesis of ylidenemalononitrile **I** from Knoevenagel reaction of benzaldehyde and malononitrile. Then, the 3-methyl-1*H*-pyrazol-5 (4 *H*)-one **II** was provided from the treatment of ethyl acetoacetate and hydrazine that would be transformed into its expected enolate form **III** under LDH/SBA/HPA catalysis. Also, the intermediated **I** can be activated by both acidic sites of the catalyst, HPA

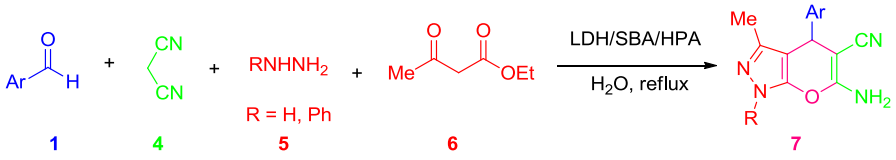

Scheme 3 Synthesis of pyranopyrazoles **7** under LDH/SBA/HPA as an extremely effective catalyst

Table 3 Optimizing the reaction conditions for the synthesis of **7a**

Entry	Catalyst amount (mg)	Solvent	Temperature	Yield (%)
1	–	Water	Reflux	Trace
2	5	Water	r.t.	10
3	5	Water	Reflux	95
4	5	CH_3CN	Reflux	50
5	5	DMF	Reflux	50
6	5	EtOH	Reflux	85
7	5	Toluene	Reflux	45
8	2	Water	Reflux	83
9	3	Water	Reflux	90
10	7	Water	Reflux	95

Table 4 [59–62]: LDH/SBA/HPA as an extremely significant heterogeneous catalyst for the formation of pyranopyrazoles

Entry	Product	R	Ar/isatin	Yield (%)[a]	Time (min)	Mp (°C) found	Mp (°C) from lit.
1	**7a**	H	C_6H_5	95	15	242–245	243–245 [59]
2	**7b**	H	4-$CH_3OC_6H_4$	87	15	206–209	208–210 [59]
3	**7c**	H	3-BrC_6H_4	89	15	219–223	220–222 [59]
4	**7d**	H	2-ClC_6H_4	92	15	245–247	246–248 [59]
5	**7e**	H	4-ClC_6H_4	95	15	231–234	233–235 [59]
6	**7f**	H	4-$NO_2C_6H_4$	89	15	250–253	249–252 [59]
7	**7g**	H	4-OHC_6H_4	88	15	223–225	224–226 [59]
8	**7h**	Ph	C_6H_5	93	20	167–169	166–168 [60]
9	**7i**	Ph	4-$CH_3OC_6H_4$	88	20	170–172	169–170 [60]
10	**7j**	Ph	4-$CH_3C_6H_4$	91	20	175–179	176–178 [60]
11	**7k**	Ph	4-ClC_6H_4	90	20	143–148	144–146 [60]
12	**7l**	Ph	4-Br-C_6H_4	85	20	183–186	184–185 [61]
13	**7m**	H	Isatin	80	15	284–287	285–286 [62]

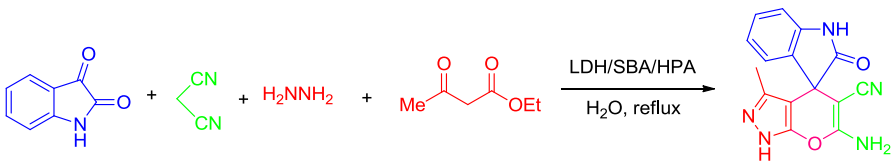

Scheme 4 Four-component reaction for the synthesis of spiro compounds

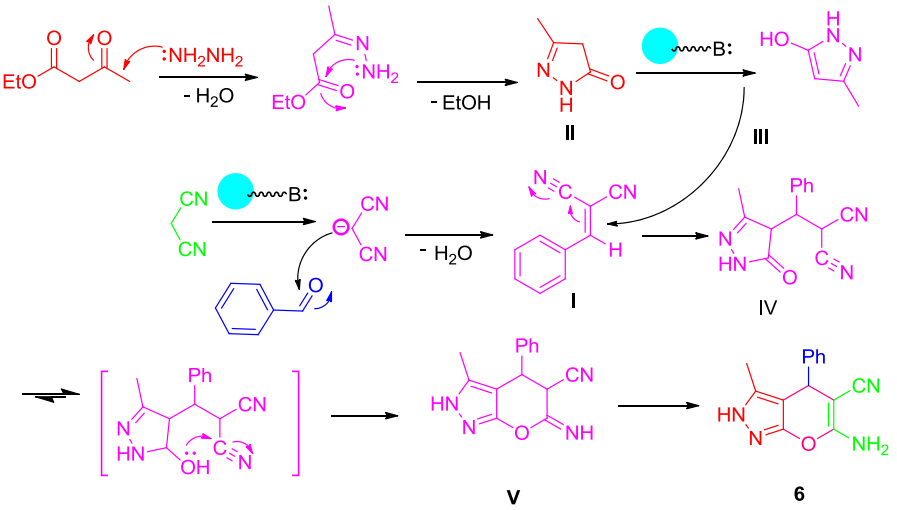

Scheme 5 Plausible mechanism for the synthesis of pyranopyrazole derivatives

and SBA-15. In the following, Michael-type reaction of **III** with the intermediate **I** provide intermediated **IV**, that experienced intramolecular cyclization by using the nucleophilic addition of enolate oxygen to the nitrile group to provide intermediate **V**. Lastly, the tautomerization of intermediate **V** afforded the corresponding pyranopyrazole **6** [62].

To demonstrate the merits of the new synthesized catalyst, its activity for the four-component reaction of benzaldehyde, ethylacetoacetate, malononitrile and hydrazine hydrate for the development of the model pyranopyrazole was compared with those reported previously (Table 5). As tabulated, compared to γ-alumina, meglumine, imidazole and phase transfer catalyst HDBAC, the ternary hybrid of LDH/SBA/HPA can mediate the reaction in shorter reaction time to furnish the desired product in higher yields. Although piperidine and isonicotinic acid led to the formation of the product in slightly lower reaction times, the yields of the product were lower than the hybrid catalyst. Additionally, the homogeneous nature of these catalysts hindered their recovery and reuse. Similarly, per-6-amino-β-cyclodextrine, which exhibited high catalytic activity, is homogeneous. Some other catalyst including nanosized magnesium oxide and magnetic Fe_3O_4 nanoparticles furnished the product in slightly higher yields. This comparison established that the hybrid system shows superior or comparative catalytic activity for a model organic transformation compared to previous reports.

Reusability of the catalyst

As simple recovery and high reusability are requisites for a heterogeneous catalyst with potential application in industry, the recyclability of the catalyst was also investigated. To this end, the yield of model pyranopyrazole was obtained in the presence of fresh catalysts. Subsequently, the catalyst was filtrated, washed with

Table 5 The comparison of the catalytic activity of LDH/SBA/HPA with formerly reported catalysts

Entry	Catalyst	Condition	Time	Solvent	Catalyst amount	Yield (%)	Ref.
1	Per-6-amino-β-cyclodextrin	Mixing, r.t.	1 min	–	0.008 mmol	> 99	[63]
2	Imidazole	80 °C	20 min	H_2O	0.5 mmol	89	[64]
3	Piperidine	r.t.	5–10 min	–	5 mol%	83	[45]
4	Magnetic Fe_3O_4 nanoparticles	r.t.	1 min	H_2O	6 mol%	97	[65]
5	Phase transfer catalyst (hexadecyl dimethyl benzyl ammonium chloride: HDBAC)	Reflux	30 min	EtOH	30 mol%	80	[66]
6	Nano-sized magnesium oxide	r.t.	10 min	MeCN	50 mg	97	[67]
7	γ-Alumina	Reflux	50 min	H_2O	30 mol%	80	[68]
8	Meglumine	r.t.	15	EtOH/H_2O (9:1)	10 mol%	90	[69]
9	Isonicotinic acid	85 °C	10 min	Solvent-free	10 mol%	90	[40]
10	LDH/SBA/HPA	Reflux	15 min	H_2O	5 mg	95	This work

EtOH and dried. Then, the reused catalyst was subjected to the next run of the same reaction. The results of the catalytic activity of the fresh and the reused catalyst up to five reaction runs are depicted in Fig. 7. As shown in Fig. 7, the catalyst could be recovered and reused for five successive reaction cycles without remarkable loss of catalytic activity. Motivated by this promising result, we also studied the leaching of HPA after five reaction runs to elucidate whether the preservation of the catalytic activity is due to the heterogeneous nature of the catalyst and low leaching of HPA. The results of ICP-AES experiments demonstrated low leaching of HPA upon reuse.

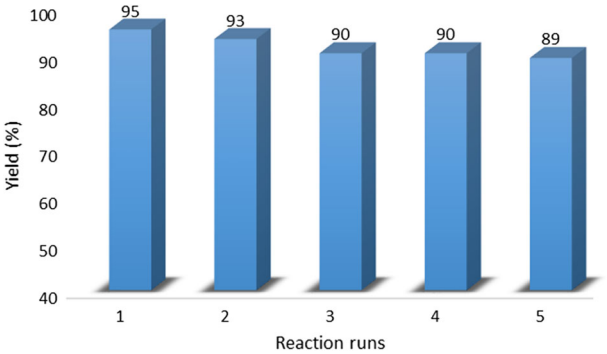

Fig. 7 Recyclability of catalyst for the synthesis of pyranopyrazoles

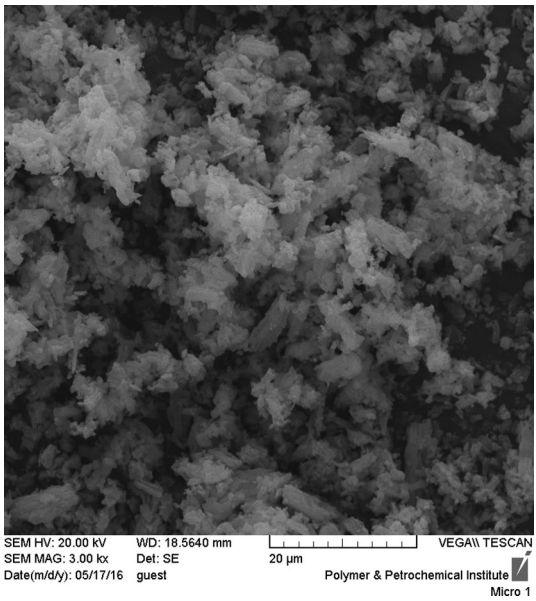

Fig. 8 SEM image of reused catalyst

This result indicated that the catalytic process does not involve leaching of HPA in the course of reaction and its re-deposition at the end of the catalytic process.

To further characterize the reused catalyst and investigate the effect of reusing on the morphology of the catalyst, the SEM image of the reused catalyst was recorded (Fig. 8) and compared with that of the fresh catalyst (Fig. 2). As depicted, the

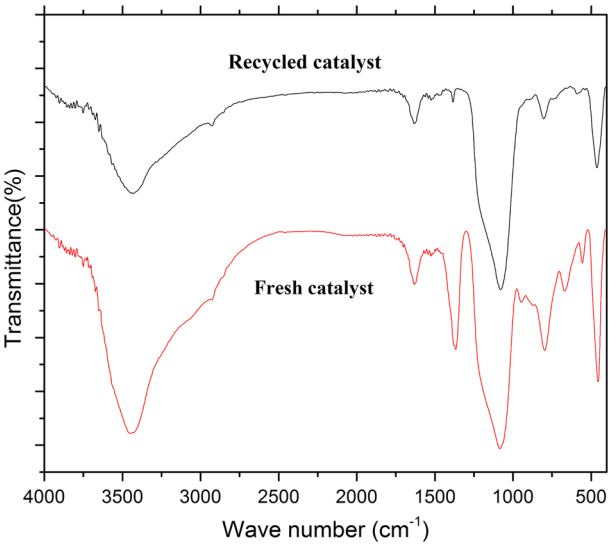

Fig. 9 FTIR spectra of fresh and recycled catalysts

reused catalyst showed more compact and aggregated morphology compared to the fresh catalyst.

The comparison of the FTIR spectra of fresh and recycled catalysts (Fig. 9) established that the recycled catalyst still showed the catalyst characteristic bands, confirming the fact that recycling did not destroy the structure of the catalyst.

Experimental

Materials

The chemicals used for the synthesis of the hybrid catalyst include Na_2CO_3 (99.9%), NaOH (ACS reagent, 98%), $Al(NO_3)_3.6H_2O$ (99%), $Mg(NO_3)_2.6H_2O$ (ACS reagent, 99%), triblock copolymer surfactant (P123), (3-aminopropyl)triethoxysilane (APTES), HCl, tetraethoxysilane (TEOS) and phosphotungstic acid ($H_3PW_{12}O_{40}$). The chemicals applied for studying the catalytic performance were phenyl hydrazine, hydrazine hydrate, malononitrile, ethylacetoacetate, isatin and aldehydes derivatives; all materials were obtained from Merck and used as received.

Synthesis of SBA-15

The silica mesoporous material SBA-15 was synthesized according to the procedure reported in the literature [49]. Typically, P123 (4.1 g) was added to deionized water (32 mL). Subsequently, a solution of 123 mL of HCl (2 M) was added to dissolve P123. After complete solvation, TEOS (10 g) was added drop-wise and the resulting mixture was stirred at 45 °C for 12 h. Finally, the solution was transferred into a Teflon-lined stain-less steel autoclave and subjected to hydrothermal treatment at 103 °C for 21 h. Upon completion and cooling, the white precipitate was filtered, washed repeatedly with deionized water and calcined at 600 °C for 6 h.

Functionalization of the SBA-15

To functionalize SBA-15, 1 g of SBA-15 was added to 100 mL of 0.01 mol L^{-1}-APTES in dry toluene. The mixture was then refluxed for 24 h, after the end of the reaction; the white precipitate was filtered, washed with deionized water and dried overnight at 100 °C.

Incorporation of HPA

To incorporate HPA onto the SBA-15, a wet impregnation method was exploited. Briefly, a solution of HPA, $H_3PW_{12}O_{40}$, (20 wt%) in acetonitrile was added drop-wise to a solution of functionalized SBA in acetonitrile. The resulting mixture was subsequently stirred vigorously overnight. Finally, the precipitate was filtered, washed with deionized water and dried overnight at 100 °C.

Synthesis of LDH

To obtain the LDH, an aqueous mixture of $Mg(NO_3)_2.6H_2O$ and $Al(NO_3)_3.9H_2O$ with an Mg-to-Al molar ratio of 2 was prepared and stirred vigorously at ambient temperature. Subsequently, a basic solution of Na_2CO_3 (0.943 mol) and NaOH (3.5 mol) was added drop-wise. Upon reaching a pH of 13, the slurry was heated at 65 °C for 18 h. Finally, the obtained precipitate was filtered, washed with deionized water and calcined at 600 °C for 8 h.

Synthesis of SBA-LDH hybrid

To a suspension of synthesized LDH in deionized water the SBA-15 (1:1 wt%) was added and the mixture was stirred vigorously for 24 h. The obtained white precipitate was dried overnight at 75 °C and subsequently dried overnight at 100 °C.

Synthesis of SBA/LDH/HPA via previous method

The previously reported synthetic procedure for SBA/LDH/HPA nanocomposite was to some extent similar to the present work. Typically, HPA-loaded SBA was synthesized according to Sections 2-2 to 2-4. The synthesis and incorporation of LDH, however, was performed in the presence of HPA-loaded SBA [48]. This catalyst is denoted as SBA/LDH/HPA/P.

Synthesis of 2,4-dihydro-3*H*-pyrazol-3-one derivatives *3a–e*

A mixture of an appropriate aldehyde (1 mmol), 5-methyl-1*H*-pyrazol-3(2*H*)-one (2 mmol) in the presence of catalytic amount of LDH/SBA/HPA as catalyst (5 mg) was refluxed in (3 ml) water for an appropriate reaction time. The progress of the reaction was monitored by TLC; upon completion, the mixture was cooled to room temperature, filtered off and the obtained solid residue was washed with H_2O. The crude products were purified by recrystallization from EtOH and H_2O.

Synthesis of pyranopyrazole derivatives *7a–m*

A mixture of hydrazine hydrate or phenylhydrazine (1 mmol), ethyl acetoacetate (1 mmol), aldehyde (1 mmol) and malononitrile (1 mmol) in the presence of a catalytic amount of LDH/SBA/HPA as catalyst (5 mg) was refluxed in water for an appropriate reaction time. The progress of the reaction was monitored by TLC; then the mixture was cooled to room temperature, filtered off and the obtained solid residue was washed with H_2O. The crude products were purified by recrystallization from EtOH and H_2O. A spiro derivative was synthesized through the similar procedure in which aldehyde was replaced with isatin.

Catalyst and product characterization

The synthesized catalyst was characterized by employing SEM/EDS, XRD, BET, elemental mapping analysis and FTIR techniques. SEM/EDS images as well as elemental mapping were recorded by a Tescan instrument, using Au-coated samples and an acceleration voltage of 20 kV. FTIR analyses were performed by using PERKIN-ELMER-Spectrum 65 instrument. Room temperature powder X-ray diffraction patterns were collected using a Siemens, D5000. CuKα radiation was used from a sealed tube. The BET analyses were carried out using BELSORP Mini II instrument. Before analysis, the SBA or the catalyst was degassed at 423 K for 4 h. Thermo-gravimetric analysis (TGA) was conducted with a METTLER TOLEDO thermo gravimetric instrument under N_2 atmosphere at a heating rate of 10 °C min^{-1} from 25 to 700 °C.

Melting points of the synthesized pyrazole derivatives were measured by using the capillary tube method with an electro thermal 9200 apparatus and FTIR spectroscopy. All known products were identified by comparison of their physical data with those of already reported authentic samples. For some selected samples, ^{1}H-NMR and ^{13}C-NMR spectra were also obtained.

Conclusion

In conclusion, a ternary hybrid catalyst comprising three active catalytic species including HPA, LDH and SBA-15 has been synthesized through a novel procedure. The catalytic activity of this novel catalyst was examined for the development of 2,4-dihydro-3*H*-pyrazol-3-one and pyranopyrazole derivatives as pharmacologically and biologically attractive molecules. Additionally, to disclose the effect of the synthetic procedure and calcination of the LDH on the catalytic activity of the catalyst, the catalytic activities of SBA/LDH/HPA and SBA/LDH/HPA/P were compared. The results demonstrated that both catalysts exhibited similar catalytic activity. The excellent catalytic performance of this catalyst was obtained in aqueous media. Some advantageous of theses procedure are cleaner reaction profiles, mild reaction conditions, excellent yields of the products, wide substrate scope, recyclability of the catalyst as well as facile experiment and separation approaches that make it a very beneficial and stimulating method for the synthesis of these compounds. Significantly, water has been considered as an eco-friendly solvent for these reactions.

Physical and spectral data for selected organic compounds

To confirm the formation of the final products, spectral data were obtained for selected products, as presented below, showing results in good agreement with previous reports [34, 63, 70], thereby proving the formation of the final products.

1. *4,4′-(Phenylmethylene)bis(3-methyl-1H-pyrazol-5-ol)* (**3a**): ^{1}H-NMR (400 MHz, d_6-DMSO): δ 2.08 (s, 6H), 4.83 (s, 1H), 7.08–7.17 (m, 3H), 7.19–7.25 (m, 2H), 11.24 (br. 4H); ^{13}C-NMR (100 MHz, d_6-DMSO): δ 10.8,

33.2, 104.7, 125.9, 127.9, 128.2, 140.2, 143.8, 161.5; IR (KBr): ν_{max}: 3296, 2971, 2500–3500, 1614, 1522, 1492, 1380, 1275, 1214, 1050, 774, 718 cm^{-1}.

2. *4,4′-((4-Hydroxyphenyl)methylene)bis(3-methyl-1H-pyrazol-5-ol)* (**3b**): ^{1}H-NMR (DMSO-d_6): δ: 2.06 (s, 6H, CH_3), 4.71 (m, 1H, CH), 6.58–6.60 (d, 2H, ArH), 6.90–6.92 (d, 2H, ArH); IR (KBr): ν_{max}: 3266, 1561, 1514, 1466, 1400, 1174, 872, 786, 731 cm^{-1}.
3. *4,4′-((4-Chlorophenyl)methylene)bis(3-methyl-1H-pyrazol-5-ol)* (**3c**): ^{1}H-NMR (400 MHz, d_6-DMSO): δ: 2.08 (s, 6H), 4.82 (s, 1H), 7.13 (d, J = 8.4 Hz, 2H), 7.27 (d, J = 8.4 Hz, 2H), 11.33 (br. 4H); ^{13}C-NMR (100 MHz, d_6-DMSO): δ 10.8, 32.6, 104.3, 128.1, 129.8, 130.4, 140.1, 142.8, 161.4; IR (KBr): ν_{max}: 2400–3500, 1601, 1532, 1491, 1203, 1172, 1091, 1015, 852, 799, 767 cm^{-1}.
4. *4,4′-((3-Nitrophenyl)methylene)bis(3-methyl-1H-pyrazol-5-ol)* (**3d**): ^{1}H-NMR (DMSO-d_6): δ: 2.11 (s, 6H, CH_3), 4.99 (ms, 1H, CH), 7.54–7.57 (d, 2H, ArH), 7.96 (s, 1H, ArH), 8.03–8.04 (s, 1H, Ar H).IR (KBr): ν_{max}: 3419, 2961, 1599, 1447, 1390, 1182, 837, 795, 764 cm^{-1}.
5. *4,4′-((4-Nitrophenyl)methylene)bis(3-methyl-1H-pyrazol-5-ol)* (**3e**): ^{1}H-NMR (DMSO-d_6): δ: 2.10 (s, 6H, CH_3), 4.98 (s, 1H, CH), 7.36–7.39 (d, 2H, ArH), 8.11–8.13 (d, 2H, ArH); IR (KBr): ν_{max}: 3419, 2961, 1603, 1510, 1442, 1346, 1178, 880, 800, 772 cm^{-1}.
6. *6-Amino-2,4-dihydro-3-methyl-4-phenylpyrano[2,3-c]pyrazole-5-carbonitrile* (**7a**): ^{1}H-NMR (DMSO-d_6): δ: 2.08 (s, 3H); 4.44 (s,1H); 6.94 (s br, 2H); 7.17–7.44 (m, 5H); ^{13}C-NMR: δ 11.4, 24.8, 70.4, 112.2, 126.3, 127.2, 129.3, 130.9, 140. 2, 143.9, 152.3, 160.0; IR (KBr): ν_{max}: 3372, 2190.74 cm^{-1}.
7. *6-Amino-4-(4-methoxyphenyl)-3-methyl-2,4-dihydropyrano[2,3-c]pyrazole-5-carbonitrile* (**7b**): ^{1}H-NMR (DMSO-d_6): δ: 2.07 (s, 3H); 3.70 (s, 3H); 4.61 (s, 1H); 7.16 (d, J = 8.7 Hz, 2H); 7.95 (d, J = 8.4 Hz, 2H); 8.61 (s br, 2H); ^{13}C-NMR: δ 11.5, 24.5, 55.4, 70.4, 114.7, 115.2, 127.8, 129.2, 14 0.5, 143.8, 153.3, 159.9, 160.0; IR (KBr): ν_{max}: 3483.78, 3255.25, 2191.7 cm^{-1}.
8. *6-Amino-4-(4-chlorophenyl)-2,4-dihydro-3-methylpyrano[2,3-c]pyrazole-5-carbonitrile* (**7e**): ^{1}H-NMR (DMSO-d_6); δ: 11.82 (s, 3H); 4.58 (s, 1H); 6.69 (s br, 2H); 7.18 (d, J = 8.1 Hz, 2H); 7.31 (d, J = 8.1 Hz, 2H); ^{13}C-NMR: 111.7, 24.4, 70.4, 112.1, 126.7, 127.6, 130.1, 134.2, 141.4, 142.1, 153.6, 159.3; IR (KBr): ν_{max}: 3380, 3281, 2193, 1622, 1454 cm^{-1}.
9. *6-Amino-3-methyl-4-(4-nitrophenyl)-2,4-dihydropyrano[2,3-c] pyrazole-5-carbonitrile* (**7f**): ^{1}H-NMR (DMSO-d_6); δ: 2.04 (s, 3H); 4.73 (s, 1H); 6.22 (sbr, 2H); 7.48 (d, J = 8.1 Hz, 2H); 8.17 (d, J = 8.1 Hz, 2H); ^{13}C-NMR: 11.4, 23.3, 70.7, 112.8, 127.9, 126.0, 130.0, 135.5,141.9, 150.4, 154.2, 160.4; IR (KBr): ν_{max}: 3383, 3272, 2198, 1620, 1451 cm^{-1}.
10. *6-Amino-4-(4-hydroxyphenyl)-3-methyl-2,4-dihydropyrano [2,3-c]pyrazole-5-carbonitrile* (**7g**): ^{1}H-NMR: δ: 2.00 (s, 3H); 4.46 (s, 1H); 6.44 (s br, 2H); 7.01 (d, J = 8.4 Hz, 2H); 6.07 (d, J = 8.1 Hz, 2H); ^{13}C-NMR: 12.0, 25.0, 71.0, 113.6, 119.5, 127.0, 130.2, 141.5, 143.8, 153.4, 154.5, 159.1; IR (KBr): ν_{max}: 878, 1271, 1368, 1583, 1645, 2222, 3056, 3350, 3410 cm^{-1}.
11. *6′-Amino-3′-methyl-2-oxo-1′H-spiro[indoline-3,4′-pyrano[2,3-c]pyrazole]-5′-carbonitrile* (**7m**): ^{1}H-NMR (DMSO-d_6, 500 MHz) δ: 1.52 (s, 3H, CH_3), 6.90

(d, J = 7.5 Hz, 1H, HAr), 6.98–7.04 (m, 2H, HAr), 7.22–7.25 (m, 3H, HAr, NH_2), 10.6 (s, 1H,NH), 12.3 (s, 1H, NH) ppm.

Acknowledgements The authors appreciate partial financial supports from Alzahra University and Iran Polymer and Petrochemical Institute. MMH is also thankful to the Iran National Science Foundation for the individual given grant.

References

1. S. Rostamnia, E. Doustkhah, RSC Adv. **4**, 28238 (2014)
2. B. Karimi, F. Mansouri, M. Khorasani, Curr. Org. Chem. **20**, 349 (2016)
3. L. Konga, X. Zhoua, Y. Yaoa, P. Jiana, G. Diaoa, Environ. Technol. **37**, 422 (2016)
4. H. Veisi, A.A. Manesh, N. Eivazi, A.R. Faraji, RSC Adv. **5**, 20098 (2015)
5. H. Veisia, M. Hameliana, S. Hemmati, J. Mol. Catal. A Chem. **395**, 25 (2014)
6. A. Wach, M. Drozdek, B. Dudek, P. Latka, P. Kustrowski, Microporous Mesoporous Mater. **226**, 433 (2016)
7. X. Song, W. Zhu, K. Li, J. Wang, H. Niu, H. Gao, W. Gao, W. Zhang, J. Yu, M. Jia, Catal. Today **259**, 59 (2016)
8. S. Sadjadi, M.M. Heravi, RSC. Adv. **7**, 30815 (2017)
9. J. Zhang, P. Jiang, Y. Shen, W. Zhang, G. Bian, J. Porous Mater. **23**, 431 (2016)
10. V. Mahdavi, M. Mardani, Res. Chem. Intermed. **41**, 8907 (2015)
11. R.L. Oliveira, W. He, R.J.M. Klein Gebbink, K.P. de Jong, Catal. Sci. Technol. **5**, 1919 (2015)
12. D. Saikia, Y.-Y. Huang, C.-E. Wu, H.-M. Kao, RSC Adv. **6**, 35167 (2016)
13. X. Sheng, Y. Zhou, Y. Yang, Y. Zhang, Z. Zhang, S. Zhou, X. Fu, S. Zhao, RSC Adv. **4**, 30697 (2014)
14. S. Sadjadi, M.M. Heravi, Curr. Org. Chem. **20**, 1404 (2016)
15. J.J. Walsh, A.M. Bond, R.J. Forster, T.E. Keyes, Coord. Chem. Rev. **306**, 217 (2016)
16. L. Hong, Y. Gui, J. Lu, J. Hu, J. Yuan, L. Niu, Int. J. Hydrog. Energy **38**, 11074 (2013)
17. Y. Zhu, M. Zhu, L. Kang, F. Yu, B. Dai, Ind. Eng. Chem. Res. **54**, 2040 (2015)
18. J. Qu, Q. Zhang, X. Li, X. He, S. Song, Appl. Clay **119**, 185 (2016)
19. S. Omwoma, W. Chen, R. Tsunashima, Y.-F. Song, Coord. Chem. Rev. **258–259**, 58 (2014)
20. S.N. Basahel, S.A. Al-Thabaiti, K. Narasimharao, N.S. Ahmed, M. Mokhtar, J. Nanosci. Nanotechnol. **14**, 1931 (2014)
21. W. Guo, Y. Zhao, F. Zhou, X. Yan, B. Fan, R. Li, Appl. Catal. A **522**, 101 (2016)
22. T. Baskaran, J. Christopher, A. Sakthivel, RSC Adv. **5**, 98853 (2015)
23. D. Pan, H. Zhang, T. Fan, J. Chen, X. Duan, Chem. Commun. **47**, 908 (2011)
24. C.O. Kappe, Acc. Chem. Res. **33**, 879 (2000)
25. M.D. Burke, S.L. Schreiber, Angew. Chem. Int. Ed. **43**, 46 (2004)
26. J. Lu, P.H. Toy, Chem. Rev. **109**, 815 (2009)
27. A. Rahmati, Z. Khalesi, Tetrahedron **68**, 8472 (2012)
28. S.V.N. Vuppalapati, Y.R. Lee, Tetrahedron **68**, 8286 (2012)
29. C.-J. Li, T.-H. Chan, *Comprehensive organic reactions in aqueous media* (Wiley, New York, 2007)
30. A. Chanda, V.V. Fokin, Chem. Rev. **109**, 725 (2009)
31. A. Schmidt, A. Dreger, Curr. Org. Chem. **15**, 1423 (2011)
32. A.N. Kost, I.I. Grandberg, Progress in pyrazole chemistry, in *Advances in Heterocyclic Chemistry*, vol. 6, ed. by A.R. Katritzky, A.J. Boulton (Academic Press, Cambridge, 1966), p. 347
33. W.S. Hamama, Synth. Commun. **31**, 1335 (2001)
34. W. Wang, S.X. Wang, X.Y. Qin, J.T. Li, Synth. Commun. **35**, 1263 (2005)
35. D. Singh, D. Singh, J. Chem. Eng. Data **29**, 355 (1984)
36. K. Niknam, D. Saberi, M. Sadegheyan, A. Deris, Tetrahedron Lett. **51**, 692 (2010)
37. D.Q. Shi, J. Chen, N. Wu, Q.Y. Zhuang, X.S. Wang, Chin. J. Org. Chem. **25**, 405 (2005)
38. K. Sujatha, G. Shanthi, N.P. Selvam, S. Manoharan, P.T. Perumal, M. Rajendran, Bioorg. Med. Chem. Lett. **19**, 4501 (2009)
39. M.N. Nasr, M.M. Gineinah, Arch. Pharm. **335**, 289 (2002)

40. M.A. Zolfigol, M. Tavasoli, A.R. Moosavi-Zare, P. Moosavi, H.G. Kruger, M. Shiri, V. Khakyzadeh, RSC Adv. **3**, 25681 (2013)
41. V.K. Ahluwalia, A. Dahiya, V.K. Garg, Indian J. Chem. Sect. B. **36**, 88 (1997)
42. N.R. Mohamed, N.Y. Khaireldin, A.F. Fahmy, A.A. El-Sayed, Der Pharma Chem. **2**, 400 (2010)
43. H. Junek, H. Aigner, Chem. Ber. **106**, 914 (1973)
44. Y.A. Sharanin, L.G. Sharanina, V.V. Puzanova, Chem. Informationsdienst, **19**, 2609–2615 (1983)
45. G. Vasuki, K. Kumaravel, Tetrahedron Lett. **49**, 5636 (2008)
46. M.M. Heravi, E. Hashemi, Y. Shirazi Beheshtiha, Sh Ahmadi, T. Hosseinnejad, J. Mol. Catal. A. **394**, 74 (2014)
47. M.M. Heravi, F. Mousavizadeh, N. Ghobadi, M. Tajbakhsh, Tetrahedron Lett. **55**, 1226 (2014)
48. S.S. Sadjadi, M.M. Heravi, V. Zadsirjan, V. Farzaneh, Appl. Surf. Sci. **426**, 889 (2017)
49. M. Hami Dindar, M.R. Yaftian, M. Hajihasani, S. Rostamnia, J. Taiwan Inst. Chem. Eng. **67**, 325 (2016)
50. A. Aouissi, Z.A. Al-Othman, H. Al-Anezi, Molecules **15**, 3319 (2010)
51. T. Baskaran, J. Christopher, T.G. Ajithkumar, A. Sakthivel, Appl. Catal. A. **488**, 119 (2014)
52. V. Fathi Vavsari, G. Mohammadi Ziarani, S. Balalaie, A. Latifi, M. Karimi, A. Badiei, Tetrahedron **72**, 5420 (2016)
53. S.K. Sharma, P.K. Kushwaha, V.K. Srivastava, S.D. Bhatt, R.V. Jasra, Ind. Eng. Chem. Res. **46**, 4856 (2007)
54. B. Wiyantoko, P. Kurniawati, T.E. Purbaningtias, I. Fatimah, Procedia Chem. **17**, 21 (2015)
55. Z. Wang, F. Liu, C. Lu, Chem. Commun. **47**, 5479 (2011)
56. S. Mallik, S.S. Dash, K.M. Parida, B.K. Mohapatra, J. Colloid Interface Sci. **300**, 237 (2006)
57. K.D. Parghi, J.R. Satam, R.V. Jayaram, Green Chem. Lett. Rev. **4**, 143 (2011)
58. K. Fan, J. Liu, X. Yang, L. Rong, RSC Adv. **5**, 37916 (2015)
59. Y. Peng, G. Song, R. Dou, Green Chem. **8**, 573 (2006)
60. M. Mirza-Aghayan, F. Saravani, A.A. Tarlani, M.S. Abaee, R. Boukherroub, Monatsh. Chem. **144**, 1699 (2013)
61. H. Sheibani, M. Babaie, Synth. Commun. **40**, 257 (2009)
62. J. Deng, L.-P. Mo, F.-Y. Zhao, Z.-H. Zhang, S.-X. Liu, ACS Comb. Sci. **14**, 335 (2012)
63. K. Kanagaraj, K. Pitchumani, Tetrahedron Lett. **51**, 3312 (2010)
64. A. Siddekha, A. Nizam, M.A. Pasha, Spectrochim. Acta Part A **81**, 431 (2011)
65. M.A.E.A.A. Ali, E. Remaily, S.K. Mohamed, Tetrahedron **70**, 270 (2014)
66. K. Ablajan, W. Liju, A. Tuoheti, Y. Kelimu, Lett. Org. Chem. **9**, 639 (2012)
67. M. Babaie, H. Sheibani, Arab. J. Chem. **4**, 159 (2011)
68. H. Mecadon, M.R. Rohman, M. Rajbangshi, B. Myrboh, Tetrahedron Lett. **52**, 2523 (2011)
69. R.-Y. Guo, Z.-M. An, L.-P. Mo, S.-T. Yang, H.-X. Liu, S.-X. Wang, Z.-H. Zhang, Tetrahedron **69**, 9931 (2013)
70. A. Vafaee, A. Davoodnia, M. Pordel, Res. Chem. Intermed. **41**, 8343 (2015)

Affiliations

Samahe Sadjadi[1] · Majid M. Heravi[2] · Vahideh Zadsirjan[2] · Vahid Farzaneh[1]

✉ Samahe Sadjadi
samahesadjadi@yahoo.com; S.Sadjadi@ippi.ac.ir

✉ Majid M. Heravi
mmheravi@alzahra.ac.ir

[1] Gas Conversion Department, Faculty of Petrochemicals, Iran Polymer and Petrochemical Institute, PO Box 14975-112, Tehran, Iran

[2] Department of Chemistry, School of Science, Alzahra University, PO Box 1993891176, Vanak, Tehran, Iran